Probing the Mechanisms of T7 RNA Polymerase Transcription Initiation Using Photochemical Conjugation of Psoralen to a Promoter†

Srinivas S. Sastry* and Barbara M. Ross

Laboratory of Molecular Genetics, Box 174, Rockefeller University, New York, New York 10021

Received July 19, 1996; Revised Manuscript Received January 7, 1997⊗

ABSTRACT: We have dissected the steps in T7 RNA polymerase transcription initiation using psoralen cross-linking. DNA templates containing cross-links at either −14/−13, −2/−1, or −4/−3 were constructed. These cross-links are within the DNA-contacting region in the initiation complex. A cross-link at −2/−1 did not affect T7 RNA polymerase binding affinity, whereas a cross-link at −14/−13 reduced binding affinity by less than 2-fold. Transcription initiation was completely blocked by cross-links at −14/−13 or at −2/−1. A cross-link at −4/−3 inhibited neither binding nor the first RNA phosphodiester bond but greatly inhibited further RNA chain extension. Circular dichroism spectroscopy revealed that DNA melting in the −4/−3 cross-link was greatly inhibited, indicating that inhibition of RNA chain extension was a melting defect. Transcription shutoff on the −14/−13 cross-link may be due to inhibition of conformational changes in the polymerase−DNA complex. Because the −2/−1 cross-link is immediately upstream of the start site (+1), open complex formation may have been completely inhibited by this cross-link, accounting for the shutoff of transcription. Thus, depending on their location, psoralen cross-links affected different steps in the initiation process. We propose that promoter melting is progressive and that melting of one or two bp upstream of the +1 site is sufficient for formation of the first phosphodiester bond while further RNA chain extension within the promoter depends on greater upstream melting of the promoter, which may be required for stabilization of the initiation complex.

T7 RNA polymerase (98.8 kDa) is one of the most extensively studied viral RNA polymerases. It is in a class of single-subunit RNAPs[1] that includes T3 and SP6 phage RNAPs (Chamberlin & Ryan, 1982; McAllister, 1993). The three-dimensional structure of T7 RNAP shows high α-helicity with a deep cleft (∼60 Å long × 15−25 Å wide × 25−40 Å deep) that accommodated ds DNA (Sousa et al., 1993; Sastry, 1996). T7 RNAP has a striking structural similarity to *Escherichia coli* DNA polymerase Klenow fragment and HIV reverse transcriptase (Joyce & Steitz, 1994, 1995). In vitro, T7 RNAP transcribes DNA without additional protein factors. Promoter complexes have been extensively characterized using footprinting, enzyme assays, mutagenesis, and gel shifts [e.g. see Chapman et al. (1988), Diaz et al. (1996), Gunderson et al. (1987), Ikeda et al. (1992a, 1993), and Muller et al. (1989)]. Elongation complexes were characterized by site-specifically blocking the path of the polymerase either with a psoralen cross-link or with a DNA-binding protein (Pavco & Steege, 1991; Sastry & Hearst, 1991a).

Psoralens are a family of photoactive compounds widely used in phototherapy of skin diseases such as psoriasis and vitilligo (Pathak & Fitzpatrick, 1992) and the sterilization of blood products (Alter et al., 1988; Lin et al., 1989, 1993). Psoralens have been applied to understand nucleic acid structure and protein−DNA interactions [for reviews, see Cimino et al. (1985), Sastry et al. (1993a), and Ussery et al. (1992)]. Psoralen-damaged DNA is a target of nucleotide excision repair (Reardon et al., 1991, 1993). Psoralens photoreact (320−380 nm UV) mostly with thymidine or uridine to form first monoadducts and then interstrand diadducts. The absorption of the first photon by psoralen results in a furanside or a pyrone side monoadduct with the 5,6 double bond of a thymidine. The furanside monoadduct can absorb a second photon to form an interstrand cross-link if a pyrimidine is available on the complementary strand of DNA. Pyrone side monoadducts cannot be driven to a cross-link because this monoadduct does not absorb photons in the 320−380 nm range [reviewed in Cimino et al. (1985)]. The high-resolution NMR structure of furanside monoadduct and cross-link showed that the local structure of the DNA was distorted (Spielmann et al., 1995a,b), but there was no significant overall bend in the DNA helix. The DNA re-assumes a canonical B-DNA conformation outside three bp of the psoralen.

Because psoralen photoadducts can be site-specifically targeted and are structurally well-characterized, they can be used to understand molecular transactions. Here, we investigated the mechanisms of T7 RNAP transcription initiation using site-specific psoralen cross-linking (or mono addition). The T7 RNAP promoter has been dissected using site-specific mutagenesis and chemical modification (Chapman & Burgess, 1987; Chapman et al., 1988; Ikeda et al., 1992b; Stahl & Chamberlin, 1978). The promoter is thought to consist of a binding domain (−16 to −5) and a melting-

† S.S.S. is a Louis B. Mayer Foundation Fellow. He thanks the Mayer Foundation for financial support. He also thanks the Hewlett-Packard Foundation for an HPLC instrumentation grant and service contracts.

* Corresponding author. Telephone: 212-327-8987. Fax 212-327-8651. E-mail: sastrys@rockvax.rockefeller.edu.

⊗ Abstract published in *Advance ACS Abstracts,* March 1, 1997.

[1] Abbreviations: bp, base pair; CD, circular dichroism; DEPC, diethyl pyrocarbonate; HPLC, high-performance liquid chromatography; RNAP, RNA polymerase; T7 RNAP, bacteriophage T7 RNA polymerase; UM, unmodified; XL, interstrand psoralen−DNA cross-link; TBE, 180 nM Tris-borate and 2 mM EDTA buffer; ss, single-stranded; ds, double-stranded; 8-MOP, 8-methoxypsoralen; nt, nucleotide; MeOH, methyl alcohol; $Mg(OAc)_2$, magnesium acetate; EtOH, ethyl alcohol.

S0006-2960(96)01793-X CCC: $14.00

initiation domain (−4 to +5) (Chapman & Burgess, 1987; Diaz et al., 1993; McAllister & Carter, 1980). Our strategy was to place psoralen cross-links in the binding and melting domains and ask the following question. How are T7 RNAP binding and initiation affected by these modifications? The results are discussed in relation to current models of T7 RNAP initiation.

MATERIALS AND METHODS

DNAs and Proteins. DNA oligonucleotides were purchased from Midland Reagent Co. (Midland, TX) and further purified by anion exchange HPLC (Sastry et al., 1992). All psoralenated and unmodified DNAs were run on preparative denaturing gels followed by electroelution of the DNA from gel slices (Sastry & Hearst, 1991a). The concentrations of DNAs were measured by UV absorbance ($\epsilon_{260} = \sim 10^4$ M^{-1} cm^{-1} per nt). Polynucleotide kinase and terminal transferase were from New England Biolabs (Beverly, MA) and Boerhinger Mannheim (Indianapolis, IN), respectively. rNTPs were purchased from Pharmacia Corp. (Piscataway, NJ) at a concentration of 100 mM. GpG (Sigma Chemical Co., St. Louis, MO) and oligonucleotides were 5′-end-labeled with the aid of [γ-^{32}P]ATP (specific radioactivity of 6000 Ci/mmol) and T4 polynucleotidekinase (Maniatis et al., 1982). 3′-End labeling was carried out with terminal deoxynucleotidyltransferase and [α-^{32}P]ddATP (Maniatis et al., 1982). T7 RNAP was prepared locally according to the procedure of Grodberg and Dunn (1988) and also by a procedure that was modified by Zawadzki and Gross (1991). The concentration of the purified T7 RNAP was determined using an ϵ_{280} of $(1.4 \pm 0.1) \times 10^5$ (Grodberg & Dunn, 1988). 8-MOP was purchased from ICN Pharmaceuticals (Irvine, CA). When needed, stock solutions at different concentrations were prepared in DMSO.

Light Sources for Irradiations. Cross-linking was carried out with a 200 W Hg(Xe) arc lamp (Oriel Corp., Stratford, CT). The lamp housing was fitted with a water filter (to eliminate IR) followed by either a dichroic mirror with reflectance of >90% in the 350−450 nm range (Oriel Corp. model 66218) or a mercury line band-pass filter centered at 365 nm (∼25% of light transmitted; 10 nm band width; Oriel Corp. model 56531). A 3.8 cm fused-silica lens was used to focus the UV beam onto the slit of a 100 μL masked quartz cuvette (1 cm path length) containing the reaction mixture. For all irradiations, the cuvette was maintained at 25−30 °C using a circulating Lauda water bath. Furan side mono addition was carried out using a 405 nm band-pass filter (Oriel corp. model 56541). This wave band generated only furanside monoadducts (Spielmann et al., 1992). Mono adducts were also prepared by photoreversal of cross-links with 254 nm light. Photoreversals with 254 nm UV light were carried out in a Rayonet photochemical reactor (Southern New England Ultraviolet Co.).

Preparation of Templates with Site-Specific Psoralen Cross-Links [*See Sastry and Hearst (1991a) for Additional Details). (1) Preparation of a 66 mer Template with a Cross-Link (or Furan Side Monoadduct) between −14T (Nontemplate Strand) and −13T (Template Strand).* A 12 mer (5′-GTATTAGGCAGC) was added to an equimolar amount (1−2 μM) of a partially complementary 16 mer (5′-GCTGCCTAATACGACT) along with 8-MOP (36 μg/mL) and mixed in 100 mM sodium acetate (pH 6.0) and 10 mM $MgCl_2$ (irradiation buffer). The mixture was held at 65 °C for 5 min and cooled to room temperature (25 °C) over a period of 3 h. The ds DNA plus 8-MOP mixture was irradiated with UVA from the Hg(Xe) source. Many experiments were carried out to achieve conditions yielding generally 50−70% cross-links. The cross-links were separated from unreacted oligos on a preparative 15% acrylamide−urea denaturing gel (Sastry & Hearst, 1991a). The cross-linked DNA was electroeluted and recovered by EtOH precipitation. The positions of the cross-links were mapped using the T4 DNA polymerase 3′ → 5′ exonuclease stop assay (Sage et al., 1993). Although there are potentially two TpA sites for 8-MOP addition in the duplex, in practice, we found that the TpA site at −14/−13 was favored compared to the other site. The two cross-links (at −14/−13 and at −17/−16) were also distinguishable by their different mobilities on denaturing gels. The cross-link at −14/−13 moved faster than the −17/−16 cross-link, probably because the former cross-link was positioned at the end of the duplex whereas the later occurred closer to the middle of the duplex. Additionally, photoreversal by 254 nm UV light and the differential oxidation of unmodified and cross-linked DNA by $KMnO_4$ were used as criteria to confirm the presence of psoralen at these positions. The purified cross-link was then ligated to form a full-length 66 mer in the presence of four other oligos (Figure 1), some of which were appropriately kinased (5′-CACTATAGGG, GATCTAG CTATTTATC-GATGGCTACGCCTCGTAGCTTCG, AGATCTCCCTAT-AGTGAGTC, and CGAAGCTACGAGGCGTAGCCATC-GATAAATAGCT).

To prepare a 66 mer template with a −2/−1 cross-link (Figure 1), we first cross-linked a 10 mer (CACTATAGGG) with a 20 mer (5′-AGATCTCCCTATAGTGAGTC). The −2/−1 cross-link was mapped using exonuclease and chemical techniques. The isolated cross-link was ligated to four other oligos, some of which were appropriately phosphorylated (5′-GTATTAGGCAGC, 5′-GCTGCCTAATACGACT, 5′-AGATCTCCCTATAGTGAGTC, and 5′-CGAAGCTAC-GAGGCGTAGCCATCGATAAATAGCT).

We have also prepared 66 mer cross-links or furanside monoadducts by first preparing either a 12 mer furanside monoadduct at −13 or a 20 mer furanside monoadduct at −1. The positions of furanside monoadducts were verified by assays described above. Furanside monoadducts were then driven to cross-links with 365 nm light. 66 mer furanside templates were constructed by ligation to appropriately kinased longer oligos. These procedures are similar to those described previously (Sastry & Hearst, 1991a; Sastry et al., 1992).

The final yields of 66 mer cross-links were 10−25% of the starting DNAs. In all cases, the 66 XLs were gel-purified after the ligations and tested for double-strandedness using restriction enzymes and photoreversal before use in the experiments described here. To obtain uniquely radiolabeled 66 XLs, we first 5′-end-labeled the 16 mer (nontemplate strand) using T4 polynucleotide kinase and [γ-^{32}P]ATP or 3′-end-labeled the 12 mer (template strand) using calf terminal deoxynucleotidyltransferase and [α-^{32}P]ddATP. The radiolabeled cross-links were ligated to cold oligos. Unmodified ds 66 mer was prepared by a cycle of heating and cooling equimolar amounts of individually synthesized 66 mer nontemplate and template strands (Figure 1).

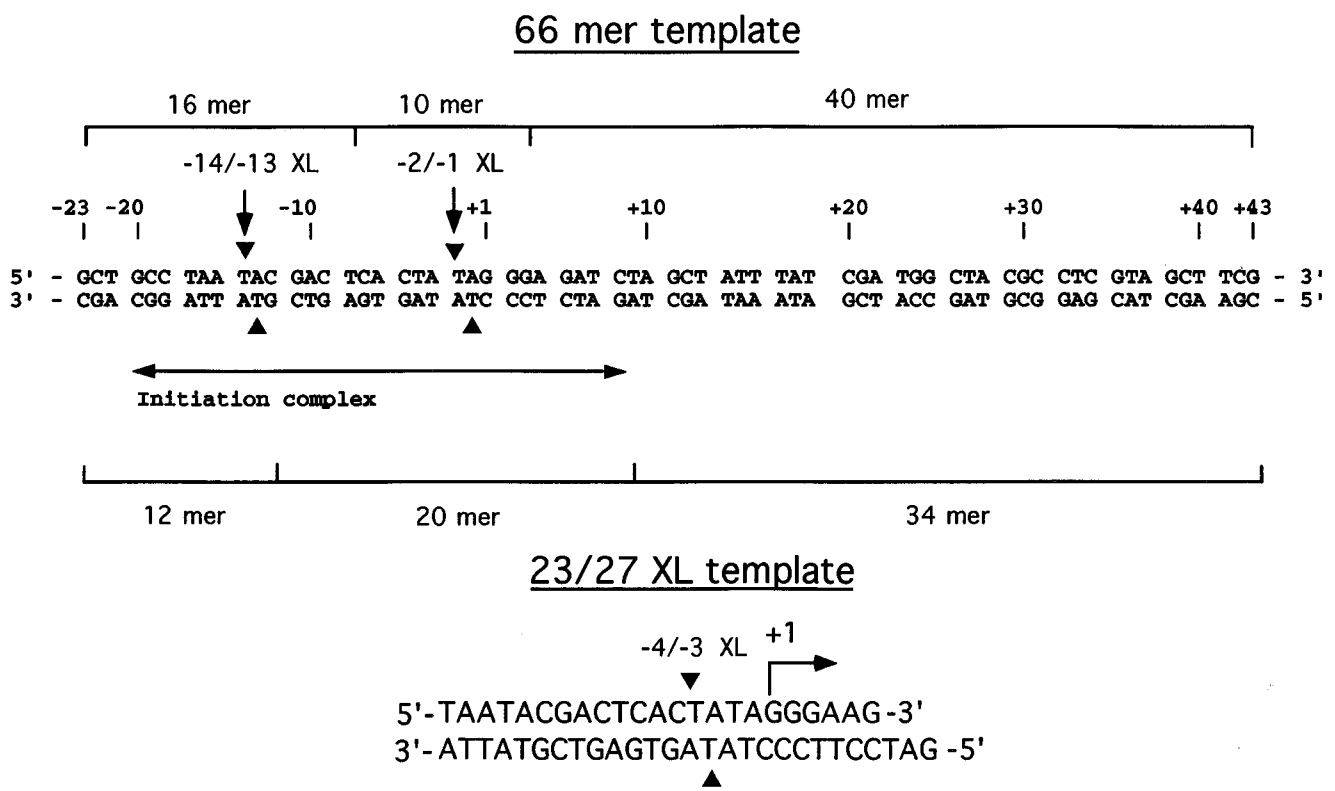

FIGURE 1: Sequence of the templates used in this work. The 66 mer templates were constructed in a modular manner by ligation of cross-links to unmodified oligos. The sizes of the individual modules are shown. The DNase I footprint of the initiation complex is shown (Shi et al., 1988b). The 23/27 XL template was constructed by direct cross-linking. The positions of site-specific psoralen cross-links are indicated by the symbols (▲, ▼).

(2) Preparation of the Template with a −4/−3 Cross-Link. A 23 mer oligo (5′-TAATACGACTCACTATAGGGAAG-3′) and a complementary 27 mer (5′-GATCCTTCCCTAT-AGTGAGTCGTATTA-3′) containing a T7 RNAP promoter sequence were commercially synthesized. Equimolar amounts of purified oligos were first mixed with 8-MOP (36 μg/mL) and annealed by heating to 70 °C and then slowly cooling to room temperature. Cross-linking was carried out using the UVA arc source fitted with the dichroic mirror (see above). Over 80% of the starting DNA was converted to cross-links. The mixture was extracted with phenol−chloroform−isoamyl alchohol (in a ratio of 25:24:1; molecular biology grade catalog no. P-3803, Sigma Chemical Co.) to remove unreacted and photomodified 8-MOP, and the DNA was precipitated with EtOH. The cross-links were HPLC-purified from unreacted and monoadducted oligos using published procedures (Sastry et al., 1992). The purified 23/27 XL DNA migrated as a single band, attesting to its homogeneity (Figure 2A).

Gel Mobility-Shift Assay. ^{32}P-labeled 66 mers (0.5 pmol) or 23/27 mers (0.5 pmol) were added to ice-cold transcription buffer [30 mM HEPES (pH 7.8, 100 mM potassium glutamate, 15 mM $Mg(OAc)_2$, 1 mM DTT, 0.05% Tween 20, and 5% glycerol (v/v) (Maslak & Martin, 1994)]. Various amounts of T7 RNAP were added to each reaction (50 μL) separately (see legends to Figures 3 and 4) and transferred to a 37 °C bath for 10 min, and glycerol (10% final) was added. The reaction mixtures (without loading dyes) were applied to an 8% acrylamide−TBE nondenaturing gel (14 cm long × 16 cm wide) that was prerun and contained fresh tank buffer. The gel was run at 5 V/cm until the xylene cyanol dye (in separate lanes) was 5−6 cm from the bottom. The gels were soaked for 20 min in 5% acetic

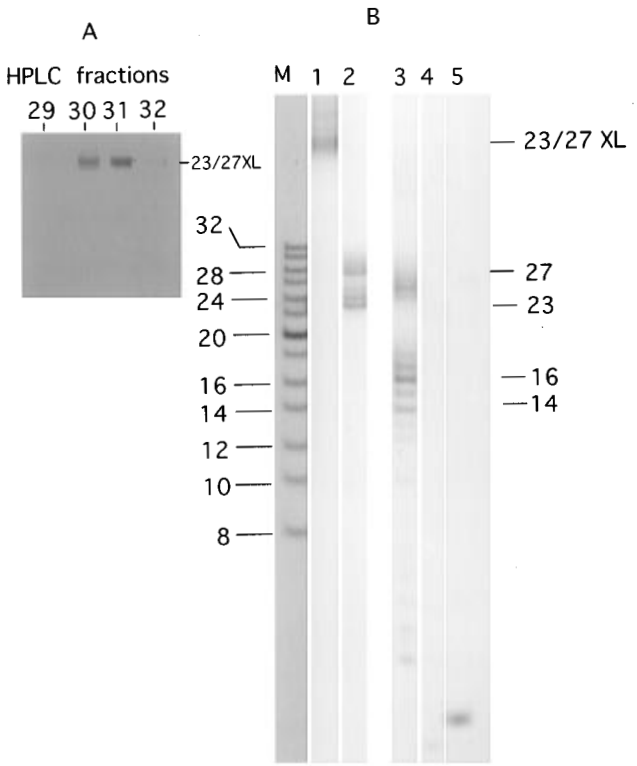

FIGURE 2: (A) Purification of the −4/−3 XL by HPLC. Fractions 30 and 31 were pooled. (B) Mapping the −4/−3 cross-link. Lane M contained 5′-^{32}P-labeled marker ladder, lane 1 purified 23/27 XL, lane 2 photoreversed 23/27 XL, and lane 3 23/27 XL digested with T4 DNA polymerase 3′ → 5′ exo in the absence of dNTPs. lanes 4 and 5 are 23/27 UM digested with T4 DNA polymerase 3′ → 5′ exo in the absence of dNTPs. In lane 4, the ^{32}P label was on the nontemplate strand, whereas in lane 5, the ^{32}P label was on the template strand.

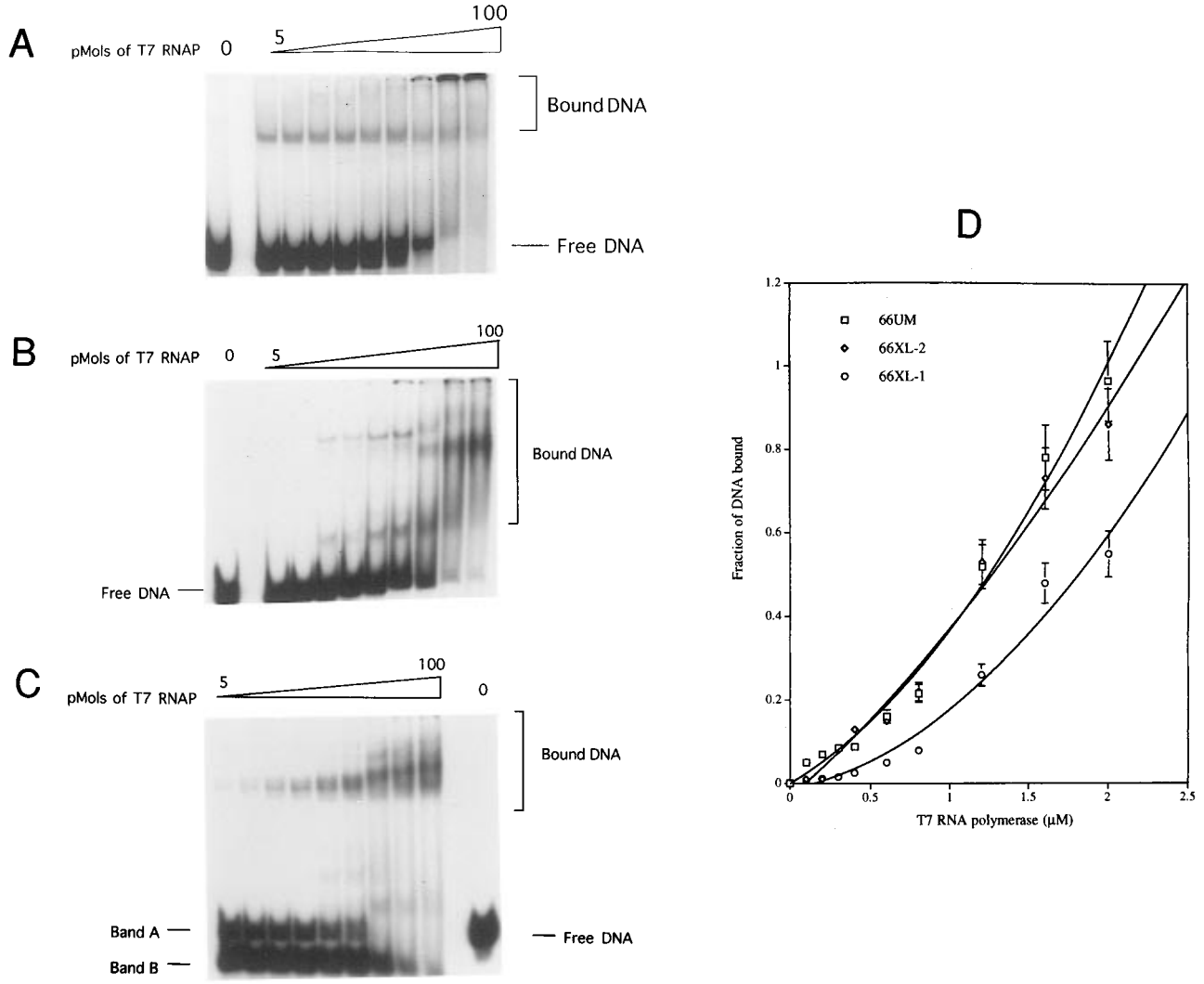

FIGURE 3: Gel-shift assay for DNA binding by T7 RNAP. The 66 mer templates ^{32}P-labeled at their 5′ ends. (A) The template was 66 UM. (B) The template was the −14/−13 XL. (C) The template was the −2/−1 XL. A constant amount of ^{32}P-labeled DNA was titrated with increasing amounts of T7 RNAP (from left to right, 5, 10, 15, 20, 30, 40, 60, 80, and 100 pmols). Lane 0 indicates that no polymerase was present. (D) Binding curves ($n = 3$). Squares are with UM, diamonds with the −2/−1 XL, and circles with the −14/−13 XL. The fraction of bound DNA (ordinates) is plotted against T7 RNAP concentration (abscissa). Each point in the graph is an average of three independent determinations.

acid, 5% MeOH, and 3% glycerol, dried, and autoradiographed with X-ray film and a phosphor screen. The fraction of bound DNA = $[BL_b/(BL_b + BL_f)]$. BL_b is the corrected band area from the storage phosphor signal representing the bound DNA, and BL_f is the band area corresponding to the free DNA in the same lane. Band areas of shifted bands were first corrected by subtracting background phosphor counts from corresponding positions in control lanes that did not contain T7 RNAP. Polymerase-bound and free DNA bands are shown in Figures 3 and 4. Band areas were obtained using the ImageQuant program of a phosphorimager.

Transcription Assay. 66 UM or 66 XLs (at a final concentration of 0.1 μM) were added to ice-cold transcription buffer containing [α-^{32}P]GpG (0.2 μM). Unlabeled GTP and ATP or all four NTPs were each present at 1 mM. In this assay, only transcripts initiated with the radiolabeled GpG will be seen [e.g. Tygarajan et al. (1991)]. Human placental RNase inhibitor (Boerhinger Mannheim Biochemicals) was present at 36 units. T7 RNAP was then added to 0.5 μM, and the reaction mixture (50 μL) was incubated at 37 °C. Aliquots (2.5 μL) of the reaction were withdrawn at different time points, mixed with 5 μL of 8 M urea−180 mM Tris-borate−10 mM EDTA, heated in a boiling water bath for 5 min, and run on a 24% acrylamide−8 M urea gel. The transcripts were visualized by autoradiography. For assays with 23/27 mer, 10 pmol of template was mixed with 50 μM GTP containing 15 pmol of [α-^{32}P]GTP (specific radioactivity of 3000 Ci/mmol) in 50 μL of transcription buffer. When needed, 8-MOP was added to a final concentration of 36 μg/mL. Transcription was started by adding 20 pmol of T7 RNAP at 37 °C. Four microliters was withdrawn at various times and processed for electrophoresis.

Circular Dichroism Spectroscopy. T7 RNAP, 23/27 XL, or 23/27 UM was dialyzed overnight at 4 °C against 10 mM potassium phosphate buffer (pH 7.8) and 10 mM $MgCl_2$. CD spectra were recorded in potassium phosphate−Mg^{2+} buffer. The solutions were clarified by centrifugation and then passed through a 0.2 μm filter to remove particulate matter. The samples were then loaded into a 1 mm path length quartz CD cell, capped tightly, and equilibrated for 15 min at the specific temperature (see Figures 8 and 9), before recording commenced. For titration experiments, a constant amount of DNA was mixed with increasing amounts

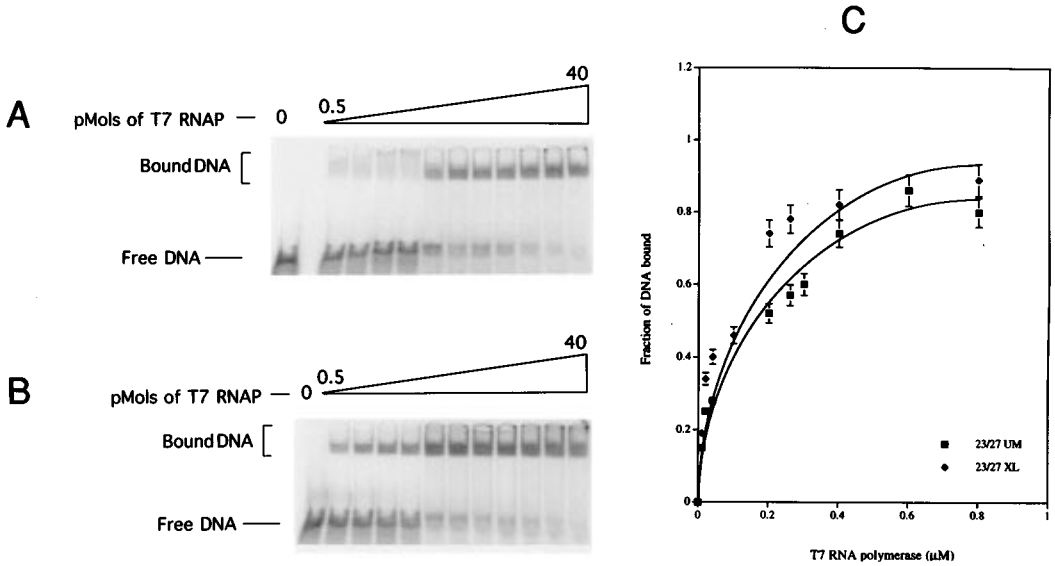

FIGURE 4: Gel-shift assay for T7 RNAP−DNA binding. (A) 23/27 UM. (B) 23/27 XL. (C) Binding curves ($n = 3$). Squares represent 23/27 UM, and diamonds represent the 23/27 XL. Each point in the graph is an average of three independent determinations.

of T7 RNAP. No precipitates were observed in gel-shift assays at the polymerase:DNA ratios tested here (e.g. see Figure 4). The final volume of all samples was kept constant at 180 μL. CD spectra were acquired using an Aviv 62DS CD spectrometer equipped with a temperature controller and interfaced with an AT&T computer. The instrument was calibrated using a two-point calibration method with (+)-10-camphorsulfonic acid. Wavelength scans were performed between 205 or 215 and 300 nm, digitized at 0.5 nm intervals, and signal averaged with an 8 s time constant. The scan rate was ~6−8 nm/min depending on the step size and time constant. Each final scan was an average of 10 repeats and corrected for baseline of buffer and smoothed. All spectra with T7 RNAP and DNA were recorded at 37 °C. The concentrations of 23/27 UM or 23 XL in CD samples were determined by UV absorbance using a Beckman DU65 UV/VIS spectrophotometer. The T7 RNAP concentrations in CD samples were determined using a bicinchoninic acid assay (Pierce Chemical Co., Rockford, IL). We used the following equation to estimate the number of bp melted by T7 RNAP, as per Reisbig et al. (1979) and Shimer et al. (1988).

$$\frac{\mathrm{Bp}_{\mathrm{melted}}}{\text{total bp}} = \frac{m_{\mathrm{e}}}{\%\Delta\theta_{275}}$$

where $\mathrm{Bp}_{\mathrm{melted}}$ is the number of bp melted by T7 RNAP (unknown quantity), total bp is the number of bp in our oligo promoter (23 bp), m_{e} is the slope of the line (negative sign was ignored) for enzyme concentrations in the range of 2−12 μM (Figure 8) (the slope was 8 for non-cross-linked promoter and 2 for cross-linked promoter), and $\%\Delta\theta_{275}$ is the percent change in ellipticity at the midpoint of the thermal transition between 37 and 67 °C (30% in Figure 9D). The underlying assumption was that promoter melting by T7 RNAP is equivalent to that of thermal melting. This assumption is supported by the similar pattern of change in ellipticity at 275 nm in Figures 8 and 9. Since our promoter oligo is only 23 bp and a typical T7 RNAP footprint covers about 20 bp (Basu & Maitra, 1986; Shi et al., 1988), we assumed that our estimate reflected the bp melted by one T7 RNAP per promoter DNA molecule.

RESULTS

Construction of Site-Specific Psoralen Cross-Linked Templates. Two types of cross-linked templates were constructed (Figure 1). The sequence of the 66 mer was almost the same as the one previously used to study elongation complexes (Sastry & Hearst, 1991a,b; Sastry et al., 1993b). Minor changes were introduced to accommodate restriction endonuclease sites. Psoralen cross-links or monoadducts were introduced at TpA sites −14/−13 or −2/−1 (Figure 1). The −14/−13 cross-link was in the binding domain, while the −2/−1 cross-link was in the melting-initiation domain. Both regions are very important for polymerase action and are within the footprint of the initiation complex (Basu & Maitra, 1986; Shi et al., 1988b; Diaz et al., 1993; Ikeda et al., 1992b; Jorgensen et al., 1991; Muller et al., 1989; Rastinejad & Lu, 1993). Both cross-links are 5′-TpA where psoralen adduction preferentially occurs (Gamper et al., 1984). Our strategy for the 66 mer templates was to first synthesize and purify on a large scale short oligo DNAs containing site-specific psoralen cross-links or monoadducts and then to ligate these to longer pieces of DNAs [see Materials and Methods and Sastry and Hearst (1991a,b), Sastry et al. (1992, 1993b), and Spielmann et al (1992)]. The full-length cross-linked templates were purified from preparative denaturing polyacrylamide gels. We constructed 1−2 nmol of extremely pure templates.

The third template (23/27 XL) has a cross-link at −4/−3. We chose this shorter core promoter oligo because we needed tens of micromolar concentrations for studying melting using CD and other techniques. The 23/27 XL DNA runs as a highly retarded band near the top of the gel (lane 1, Figure 2B), which is a characteristic of psoralen-cross-linked DNA. Photoreversal of the cross-link with 254 nm UV light revealed the 23 mer and 27 mer strands and the respective monoadducts, which migrate about one nucleotide slower than free ss DNAs (note that both strands are ^{32}P-labeled at the 5′ ends; Figure 2, lane 2). Digestion with T4 DNA polymerase 3′ → 5′ exo followed by photoreversal produced

a cluster of bands predominantly 14−16 nts long (lane 3, Figure 2B). This pattern is consistent with the interpretation that the T4 exo activity stopped one nt prior to the cross-link on the template strand because of the cross-link between −4 and −3 (accounting for the 14 nt fragment). On the nontemplate strand, the exo activity stopped at −2T (one nt prior to −3), accounting for the 16 nt fragment. The 15 mer and the 17 mer are monoadducts resulting from photoreversal. Digestion of non-cross-linked duplex with T4 DNA polymerase 3′ → 5′ exo generated two or three nts (lanes 4 and 5, Figure 2B), consistent with the limit product of the enzyme when there is no blockage (Kornberg & Baker, 1992) .

A Cross-Link at −14/−13 Inhibits T7 RNAP Binding to a Small Extent, but Cross-Links at −2/−1 or at −4/−3 Do Not Inhibit Binding. Figure 3A−C shows gel shifts of 66 UM, −14/−13 XL, and −2/−1 XL templates complexed with T7 RNAP. With increasing polymerase concentration, a larger fraction of UM or XL DNA was complexed. Both templates formed discrete complexes at lower polymerase concentrations, whereas at higher concentrations, multiple complexes were seen. At high T7 RNAP concentrations, some complexes did not enter the gel while others appeared smeary. Competition experiments with calf thymus DNA suggested that the discrete bands are the specific complexes [see also Muller et al. (1988)]. With −2/−1 XL, a new band was observed (Figure 3C, band B) that migrated faster than the starting material (band A). Photoreversal indicated that band B DNA contained both strands. We believe that band B is a free DNA isomer induced by the polymerase and is stabilized by the psoralen cross-link (data not shown). Since our focus was the mechanism of transcription, no further attempts were made to characterize band B DNA.

The fractional saturation of DNA as a function of polymerase concentration was quantitated (see Materials and Methods). Polymerase binding was inhibited by less than 2-fold by the cross-link at −14/−13, while the −2/−3 cross-link did not inhibit binding (Figure 3D). Since the DNA concentration is extremely small relative to that of the protein, the macroscopic equilibrium binding constant (K_b) was equivalent to the polymerase concentration at which half-maximal saturation of the DNA occurred. For UM or −2/−1 XL, the K_b was $\sim 1.2 \times 10^6$ M^{-1}, whereas for −14/−13 XL, it was slightly larger, $K_b \sim 1.7 \times 10^6$ M^{-1}. With the −4/−3 XL template, at lower T7 RNAP concentrations, a discrete complex was seen compared to UM. At higher T7 RNAP concentrations, both DNAs contained discrete complexes (Figure 4A,B). We believe that the −4/−3 XL−T7 RNAP complex is a "less-open DNA conformation" compared to the UM−T7 RNAP complex (see CD spectra, below). The estimated binding constants (defined above) for the −4/−3 cross-link and UM were the same within experimental errors ($K_b \sim 0.17 \times 10^6$ M^{-1}). The macroscopic equilibrium binding constant reported here compares favorably with that reported by others for short oligonucleotide templates (Diaz et al., 1996). The different shapes of the binding curves in Figures 3D and 4C may be due to the presence of additional upstream sequences in the longer templates compared to the shorter templates (Figure 1). The sequences may have introduced changes in specific T7 RNAP recognition modes. In support of this point, we note that DNase I footprints showed contacts up to −20 (Basu & Maitra, 1986).

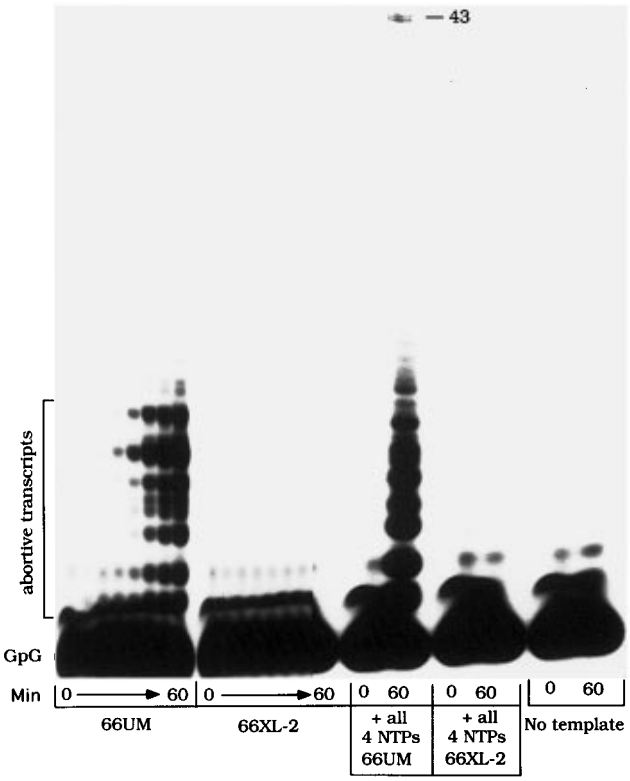

FIGURE 5: Inhibition of initiation of transcription by the −2/−1 cross-link. The time course of transcription initiation is shown. For UM and XL templates, lanes from left to right represent aliquots of the reaction at 0, 0.5, 1, 2, 5, 15, 30, and 60 min. In other lanes, 0 and 60 indicate aliquots from the reaction mixture before and 60 min after the addition of polymerase, respectively. α-^{32}P-labeled GpG was the initiating dinucleotide.

Transcription Initiation Is Completely Blocked by −14/−13 and −2/−1 Cross-Links. Under the assay conditions employed here (see Materials and Methods), only transcripts initiated with [α-^{32}P]GpG are visualized [see Tygarajan, et al. (1991)]. On 66 UM, the enzyme stalls at +6 in the presence of ATP and GTP. However, up to eight or nine nt transcripts are observed (Figure 5). This is probably because, after incorporation of the dinucleotide [α-^{32}P]GpG at the +1 and +2 (or +2 and +3), the enzyme may undergo slippage at the +3C position (see below for slippage assay), incorporating two or three additional GMP residues before moving forward. The term "abortive transcripts" (Figure 5) is used merely to suggest that short transcripts were produced probably in an abortive manner (McClure, 1985). On the −2/−1 XL template, transcription initiation was completely shut off, even after prolonged incubation with all four NTPs, whereas on UM, the expected 43 mer runoff was synthesized. The same result was seen with −14/−13 XL and furanside monoadducts at these positions (not shown). Using only [α-^{32}P]GTP, no initiation was observed either (not shown).

Transcription Initiation Is Not Blocked by a Cross-Link at −4/−3. Two types of assays were used: the "abortive cycling" assay (defined here as synthesis in the presence of GTP plus one or more NTPs) and the poly(G)-ladder synthesis assay (where only GTP is present) [e.g. see Gross et al. (1992), Ling et al. (1989), Martin et al. (1988), and Sousa et al. (1992)]. In the poly(G)-ladder assay, T7 RNAP synthesizes RNA that extends to ∼14 nts and abruptly tapers off (Figure 6A). Poly(G)-ladder is believed to be due to reiterative slippage synthesis at the three Cs on the template strand (+1 to +3; Martin et al., 1988) without much physical

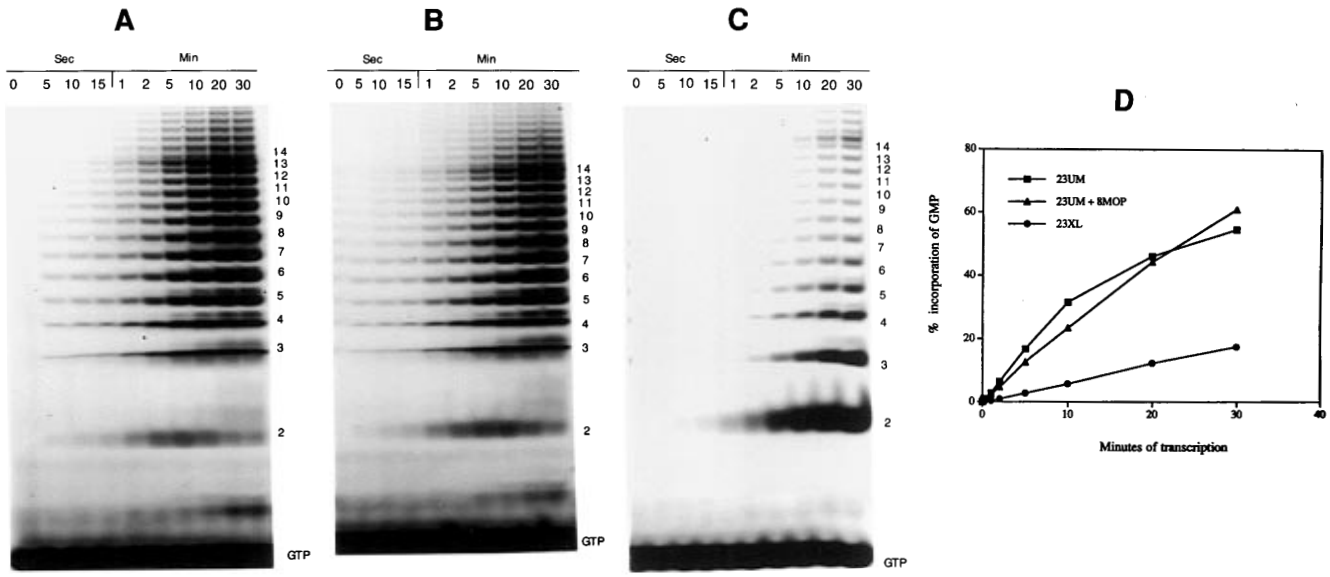

FIGURE 6: Kinetics of G-ladder synthesis on the 23/27 mer duplex (A) in the absence of 8-MOP with 23/27 UM, (B) in the presence of 8-MOP with UM, and (C) with the −4/−3 XL. The rate of sampling of the transcription reaction is indicated at the top of the gels. The numbers on the right-hand side indicate the length of the ladder deduced by counting the distinct bands on the gel. The panels shown here were run on identical 24% denaturing gels. (D) A plot illustrating the inhibition of the synthesis of greater than pppGpG. The percent GMP incorporation was calculated from the radioactivity in the gel strips not including the dinucleotide.

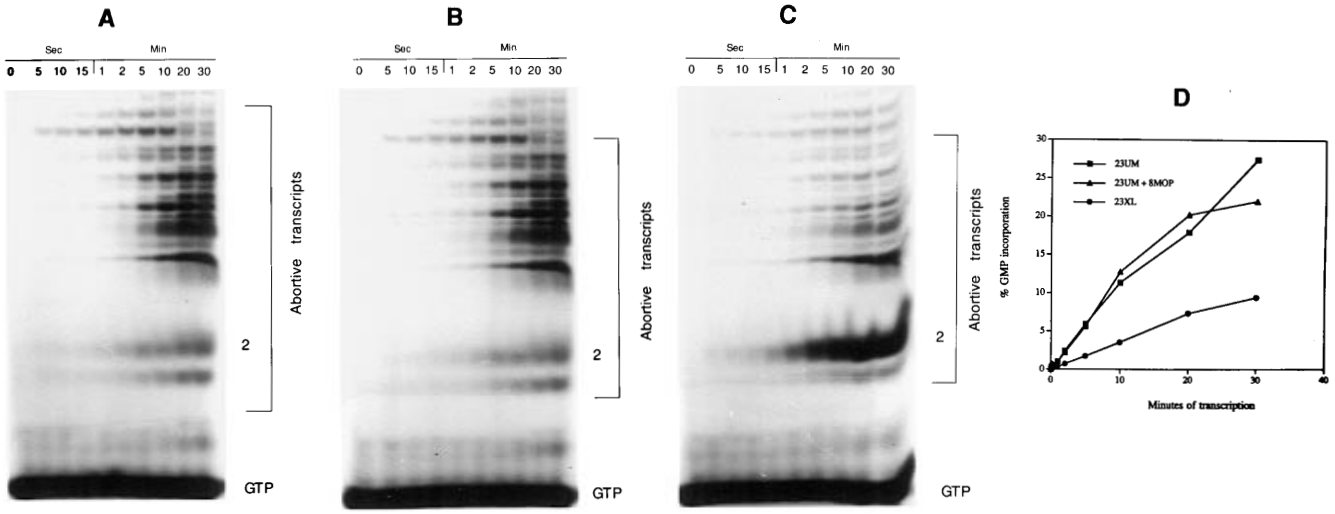

FIGURE 7: (A−D) Kinetics of the synthesis of short RNAs with GTP and ATP (A) in the absence of 8-MOP with UM, (B) in the presence of 8-MOP with UM, and (C) with the −4/−3 XL. The rate of sampling of the transcription reaction is indicated at the top of the gels. The 2 mer RNA is indicated on the right. All the panels shown here were run on the same gel. The gel photographs are phosphor images of the gel. (D) A plot illustrating the inhibition of synthesis of >2 mer. The percent GMP incorporation was calculated from the radioactivity in the gel strips that did not include the dinucleotide.

translocation of the active site of the enzyme, as represented by the 3′-OH of the transcript. On the other hand, during abortive cycling with GTP and ATP, the active site of the enzyme can move up to +7 from the start site (+1 arrow in Figure 1) and the short transcripts are thought to be released from T7 RNAP ternary complexes without enzyme dissociation from the template. Ternary complexes in the slippage mode may be more stable than those in the abortive mode (Borukhov et al., 1992; Sousa et al., 1992).

In contrast to −2/−1 XL or −14/−13 XL, the −4/−3 cross-linked template supported initiation (Figures 6C and 7C). No synthesis occurred in the absence of template (not shown). Interestingly, the first phosphodiester bond (pppGpG) was not blocked, but subsequent extension to poly(G) was progressively inhibited (Figure 6C). A similar result was seen in the abortive initiation assay (Figure 7C). To reinforce this point, we counted the ^{32}P in the dinucleotide (pppGpG) fraction separately from that in the longer transcripts. The rate of GMP incorporation in the poly(G) ladder (i.e. greater than pppGpG) was ∼6−7-fold less with the −4/−3 cross-linked template compared to that with the non-cross-linked template (Figure 6D). In the abortive mode, GMP incorporation with cross-linked template was 3−4-fold less than that with unmodified template (Figure 7D). Conversely, the amount of labeled pppGpG at 30 min was 5−6-fold greater with the −4/−3 cross-linked template compared to that with the unmodified template. These results demonstrate that the −4/−3 cross-link does not inhibit first phosphodiester bond formation but further extension of the RNA chain is inhibited (see Discussion).

Transcription Initiation Is Not Inhibited by Noncovalent Psoralen. Why does psoralen cross-linking shut off (or inhibit) transcription initiation? Is this because of the increased stabilization of the DNA helix due to favorable

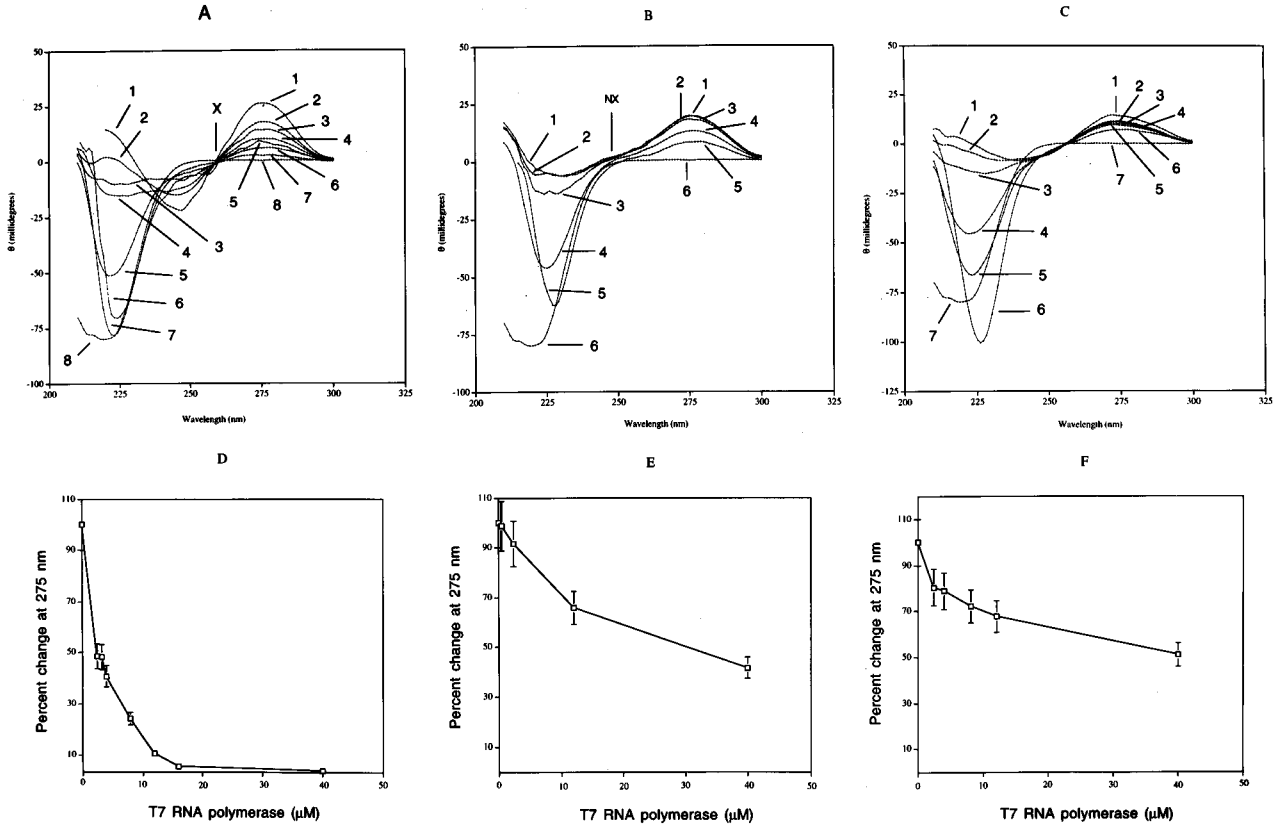

FIGURE 8: CD spectroscopy of T7 RNAP−DNA complexes. (A) Curve 1 is free promoter at 8 μM. Curves 2−7 are T7 RNAP at 2, 4, 8, 12, 15, and 40 μM, respectively. Curve 8 is with free T7 RNA polymerase at 40 μM. (B) Curve 1 is cross-linked promoter at 7 μM. Curves 2−5 are T7 RNAP at 1.5, 3.5, 12.0, and 40 μM, respectively. Curve 6 is with free T7 RNA polymerase at 40 μM. (C) Curve 1 is nonpromoter at 5 μM. Curves 2−6 are T7 RNAP at 2.0, 3.0, 5.0, 8.5, and 40 μM, respectively. Curve 7 is with free T7 RNA polymerase at 40 μM. (D−F) The change in θ_{275} is expressed as a percentage of free DNA value (taken as 100%). X and NX indicate the points of crossover from a positive to a negative sign.

enthalpy associated with intercalation of the planar psoralen (Kao, 1984; Nelson & Tinoco, 1984)? Or is "open complex" formation prevented because the two DNA strands are "tied up" ? To answer these questions, we compared initiation with covalently and noncovalently intercalated/stacked psoralens. Psoralen is intercalated in cross-linked as well as in non-cross-linked DNA (Spielmann et al., 1995a,b). We added saturating amounts of free 8-MOP (36 μg/mL; 23 psoralens per 23 bp DNA) to 23/27 bp unmodified promoter. Because intercalators are thought to obey the "nearest-neighbor exclusion principle" (Saenger, 1984), noncovalently bound psoralens might be intercalated between every second bp. Assuming a random mode of intercalation at equilibrium, there are at least two sets of DNA molecules in the population that have psoralen intercalated between alternating base pairs (other combinations also occur). 8-MOP did not inhibit transcription initiation (Figures 6B and 7B). Some psoralens may be displaced during T7 RNAP binding and initiation. Because T7 RNAP was cross-linked to DNA *via* bound psoralen in complexes (Sastry, 1996), we believe T7 RNAP binding may not be impaired. However, the observed transcription may have occurred by the displacement of noncovalently bound psoralen. This is not possible with covalently bound psoralen in the form of cross-links. Thus, transcription inhibition on cross-linked DNA may be due to a melting defect (i.e. inhibition of open complex formation).

CD Spectroscopy of Open Complexes. We used CD to demonstrate that inhibition of RNA chain extension on the −3/−4 cross-link was due to a melting defect. The CD of promoter DNA (Figure 8A, curve 1) is characteristic of B-DNA, viz., an almost equal magnitude of positive and negative ellipticities above 230 nm and a crossover point (X) at the absorption maximum of 260 nm (Ivanov et al., 1973). When a fixed concentration of promoter DNA was titrated with T7 RNAP, changes in ellipticity at 275 nm corresponding to DNA occurred (Figure 8A) (Cantor & Schimmel, 1980). These changes indicated DNA melting [e.g. see also Butzow et al. (1991), Reisbig et al. (1979), and Shimer et al. (1988)] because heating the promoter DNA accomplished the same result as increasing the polymerase concentration (viz., decrease in θ_{275}; compare Figures 8A,D and 9A,D). The decrease in positive ellipticity at 275 nm bore the hallmark of unwinding of the DNA bases at higher temperatures (Johnson et al., 1981; Usattyi & Shlyakhatenko, 1973; Reisbig et al., 1979; Scaria et al., 1995). Open complex formation was dependent on polymerase concentration (Figure 8D), similar to the results from *E. coli* RNAP (Buc & McClure, 1985; McClure, 1985). By the same criteria, there was very limited melting of cross-linked promoter (Figures 8B,E and 9B,E). At the highest T7 RNAP concentration, about 45% less change in the 275 nm CD band compared with that of non-cross-linked promoter was observed (Figure 8E *vs* Figure 8D). Figure 8C shows the CD of T7 RNAP interacting with a nonpromoter DNA (5′-GATCGCTCCCGGGTACCGAGCTCG-3′). T7 RNAP-induced melting is approximately the same for cross-linked promoter and nonpromoter (Figure 8E,F). However, temperature-induced melting of nonpromoter DNA is similar to that of promoter DNA as compared to that of cross-linked DNA (compare panels F and D of Figure 9).

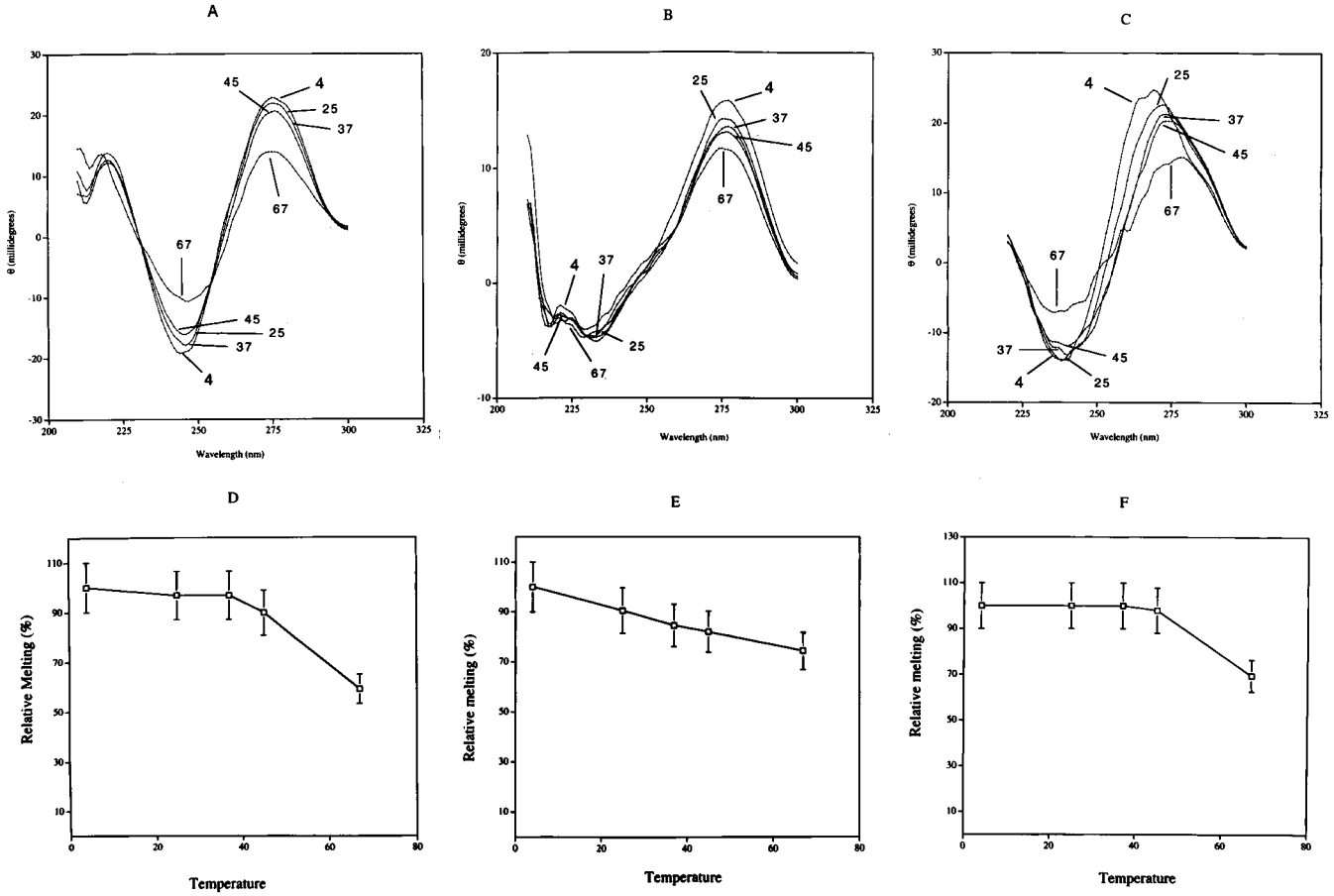

FIGURE 9: Thermal denaturation curves for 23/27 UM (A), the 23/24 XL (B), and nonpromoter (C). Curve numbers indicate the temperature at which the spectra were taken. (D−F) The change in θ_{275} is expressed as a percentage of the value at 4 °C (taken as 100%).

Previous workers estimated the number of bp disrupted by *E. coli* RNAP using UV spectroscopy (Reisbig et al., 1979; Shimer et al., 1988). Here, we used a similar approach (see Materials and Methods). We estimated that ~6 bp were disrupted by T7 RNAP per promoter molecule, whereas in the cross-linked promoter, only 2 bp were disrupted. These results indicated that dinucleotide synthesis (Figures 6C and 7C) occurred even though only two bp were disrupted in the cross-link. Presumably, extension to a G-ladder required greater bp disruption, as is the case with non-cross-linked promoter. Our estimate of the melted region for unmodified promoter was roughly equivalent to that in previous reports (Muller et al., 1989; Osterman & Coleman, 1981) and to that using sensitivity to $KMnO_4$.[2]

The CD of cross-linked promoter by itself has an unusual shape compared with that of non-cross-linked promoter (Figures 8B and 9B compared with Figures 8A and 9A), indicating that psoralen cross-linking induces a significant departure from the canonical B-DNA. The crossover point (NX) for the cross-linked promoter is blue-shifted to 246 nm compared to the unmodified promoter whose crossover point is at the conventional 260 nm. The magnitude of positive transition between 250 and 300 nm is 3.5 times greater than the relatively smaller negative transition (215 to 247 nm; Figure 9B). In conventional B-DNA, the positive and negative CD bands are of approximately equal magnitude (Figure 9A). Moreover, between 215 and 230 nm for promoter DNA (B-DNA), the CD has a positive sign whereas the CD for the cross-linked promoter has a negative sign (Figures 8B and 9B *vs* Figures 8A and 9A). The CD of cross-linked promoter in Figures 8B and 9B is reminiscent of the CD of A-DNA (Ivanov et al., 1973), which has implications for our results on binding and initiation (see Discussion).

[2] Unpublished results.

DISCUSSION

Prokaryotic transcription initiation is a complex set of transitions (eq 1) [reviewed in McClure (1985)]. The recognition of the promoter (P) by RNAP (R) leads to the formation of closed complexes (RP_c).

$$R + P \underset{k_{-1}}{\overset{k_1}{\rightleftharpoons}} RP_c \underset{k_{-2}}{\overset{k_2}{\rightleftharpoons}} RP_o \xrightarrow{NTPs} RNA \qquad (1)$$

The DNA in the closed complexes is double-stranded. The closed complexes isomerize to open complexes, in which the DNA is partially melted (RP_o) [for review, see deHaseth and Helmann (1995)]. In the presence of NTPs, RP_o begins synthesis of RNA. For *E. coli* RNAP, there are intermediates (RP_{o1}, RP_{o2}, etc.) between RP_c and RP_o, and probably several types of complexes at each step depending on the promoter, the temperature, and the ionic strength [for example, see Buc and McClure (1985), Cowing et al. (1989), Kovacic (1987), Krummel and Chamberlin (1989), Mecsas et al. (1991), Roe et al. (1985), Spassky et al. (1985), and Suh et al. (1992a,b)]. For T7 RNAP, although it has been implicitly accepted that the overall initiation reaction follows eq 1, so far RP_c and RP_o have not been experimentally separated and no inter-

mediates have been identified. Further, any open complex model of T7 RNAP initiation may have to account for the fact that some partially single-stranded promoters are as effective as fully double-stranded promoters (Maslak & Martin, 1993) and that initiation is faster than complete strand opening (Sastry & Ross, 1996).

The T7 RNAP promoter consists of 23 bp (−17 to +6) of a highly conserved sequence (Chamberlin & Ryan, 1982; Dunn & Studier, 1982, 1983). Base analog substitutions suggested that certain changes in functional groups in the DNA grooves were detrimental to transcription while others were not (Stahl & Chamberlin, 1978). Subsequently, several T7 promoter point mutations that reduced polymerase binding but did not affect transcription were mapped (Chapman & Burgess, 1987; Chapman et al., 1988; Ikeda et al., 1992b). These results suggested that the T7 RNAP promoter was organized into two functional domains: a binding domain (−16 to −5) and a melting-initiation domain (−4 to +5) (Chapman & Burgess, 1987; Diaz et al., 1993; McAllister & Carter, 1980). Here, we studied the effects of psoralen photoadditions at three separate sites (−14/−13, −2/−1, and −4/−3) in the promoter using a combination of biochemical and physicochemical methods.

The NMR structure of psoralen-cross-linked DNA showed that the psoralen moiety is intercalated between the base pair steps (Spielmann et al., 1995a,b). Although the base pairs above and below the psoralen appear somewhat buckled, H bonding is not completely disrupted [see Figure 2 in Spielmann et al. (1995b)]. In the case of the cross-link, there may be increased solvent accessibility. The DNA helix shows a very minor bend of ∼8°. In both adducts, the helix is unwound by ∼28° and the repeat length is altered (11 bp repeat as in A-DNA *vs* 10.5 bp in standard B-DNA), indicating intercalation of psoralen. Consistent with NMR, our CD spectra of −4/−3 cross-linked promoter revealed that the altered conformation is somewhat reminiscent of A-DNA. The DNA returns to normal B-form outside three bp of the psoralen. Due to the change in the hybridization of the C5−C6 orbitals from sp^2 to sp^3, the C5−CH_3 and C6−H point away from the psoralen but still point into the major groove. The 5′ bases above and below the psoralen stack onto the CH_3 of the photoalkylated dT, coplanar with the pyrimidine ring.

(1) Psoralen cross-links at −2/−1 and at −4/−3 do not inhibit polymerase binding, while the −14/−13 cross-link inhibited binding to a very small extent. Footprinting showed that −14/−13, −4/−3, and −2/−1 sugars on both strands were protected from hydroxyl radical attack, indicating that these bases were contacted by T7 RNAP (Muller et al., 1989). Mutagenesis of −14 did not affect transcription, while alterations at −13 decreased transcription to some extent (Diaz et al., 1993). Base substitutions and modification in this region generally decreased polymerase binding (Jorgensen et al., 1991). Mutagenic alterations at −2, −3, and −4 reduced transcription initiation dramatically (Chapman & Burgess, 1987).

Modifications resulting from psoralen cross-linking are quite different from those produced by base substitutions, deletions, additions, methylation, or ethylation. The latter are microscopic changes in the DNA. As indicated by NMR and CD, psoralen photoaddition results in macroscopic alterations in DNA conformation, and as such, our approach is complementary to conventional base mutagenesis. Our cross-linking results are sometimes in agreement with and in other instances not in agreement with current models of T7 RNAP transcription initiation. If T7 RNAP recognizes the promoter by a "direct read-out" of the functional groups in the DNA major and minor grooves, and if binding specificity is not due to any specific conformational features of the promoter (Maslak et al., 1993; Raskin et al., 1992; Schick & Martin, 1995), one can see why psoralen cross-links do not greatly affect binding. In cross-links, all the necessary functional groups (H-bond acceptors and donors) are still available for direct read-out even though the overall DNA conformation is different. In this sense, our results support the current model for promoter binding. Geometrical alterations in −2/−1 or −4/−3 cross-links may not inhibit recognition because dynamic changes in T7 RNAP may compensate for changes in DNA ("induced-fit"). In addition, because these cross-links are in the "melting" domain, binding is unaffected. The small decrease (1.5-fold) in affinity for the −14/−13 cross-link may be due to a more severe conformational alteration in the binding domain. No published information is available regarding sequence-context effects on the structure of psoralen cross-links.

(2) It was surprising that the −14/−13 cross-link repressed transcription. Inhibition of melting may not be the case here because this cross-link is not in the melting domain but is in the binding domain. It is also unlikely that the polymerase made strong contacts with the psoralen moiety itself. The psoralen does not have charged, accepting, or donating functional groups (except for the oxygen atoms). Instead, we believe that the −14/−13 cross-link may have prevented a crucial conformation change(s) in the polymerase−DNA complex that preceded DNA melting. In agreement with our results with the −14/−13 cross-link, a recent report suggested that T7 RNAP contacted −13 (Ujvari & Martin, 1996). The cross-link at −2/−1 shut off transcription, while the cross-link at −4/−3 did not. Since CD with the −4/−3 cross-link showed that melting was defective but not totally abolished (Figure 8B,E), it is quite likely that the −2/−1 cross-link exhibited a more dramatic melting defect, leading to a complete shutoff of transcription because the −2/−1 cross-link is immediately upstream of the +1 start site. Neither binding (as measured by K_b in Figure 4) nor initiation (as measured by the amount of dinucleotide pppGpG in Figures 6 and 7) was affected by the −4/−3 cross-link. However, RNA longer than a dinucleotide was dramatically reduced (Figures 6 and 7). Hence, neither RP_c formation nor $RP_c \rightarrow RP_o$ isomerization in eq 1 was inhibited by the −4/−3 cross-link. This suggested that there were rate-determining steps *following* formation of the first bond (pppGpG) that required greater promoter melting than that exhibited by the −4/−3 cross-link.

On the basis of our work with the various cross-links, we propose the following mechanism. There is a conformational step(s) after polymerase binding preceding melting (RP_o) for initiation. This step is defective in the −14/−13 cross-link. $RP_o \rightarrow$ RNA (eq 1) transition consists of more than one step, a rapid step 1, with a short burst of a two bp melted region near +1 wherein the first bond occurs (dinucleotide, pppGpG). This is followed by step 2, with a larger upstream−downstream melted region wherein a steady-state lengthening of the transcript occurs. Step 2 was inhibited by the −4/−3 cross-link, whereas step 1 may not have occurred with the cross-link at −2/−1. In a recent work

using fluorescence spectroscopy, we reported that during open complex formation at 37 °C −1 bp was disrupted quickly ($\sim 2-3 \times 10^7\ M^{-1}\ s^{-1}$), which may account for the absence of a lag time for initiation of RNA synthesis (Sastry & Ross, 1996). The observed total shutoff of transcription initiation by the −2/−1 cross-link agrees with this model. For *E. coli* RNAP, others (Buc & McClure, 1985) have identified a rate-determining step following promoter melting. Some have proposed at least two open complexes for *E. coli* RNAP depending on Mg^{2+} stoichiometry (Suh et al., 1992a,b). A two-open-complex model has been proposed for *Bacillus subtilis* RNAP (Juang & Helmann, 1995).

Maslak and Martin (1993) suggested that DNA melting is not a barrier for T7 RNAP initiation. Our result with the −4/−3 cross-link showing first bond formation (Figures 6 and 7) coupled with very little melting (Figure 8) agrees with their proposal only so far as first bond formation is concerned. Extrapolating from partially ss promoters to fully ds promoters may be difficult [cf. Maslak and Martin (1993)]. T7 RNAP may contact fully ds promoters in a qualitatively different manner compared to partially ss promoters (especially with large gaps) because the DNAs are structurally different. Indeed, recent evidence indicates that binding and stability of complexes are different on partially ss and fully ds templates (Diaz et al., 1996; Jia et al., 1996) and that different subdomains of the polymerase may be involved in interactions with ds and ss DNAs (Sastry, 1996).

Finally, our work has implications for the biological effects during phototherapy with psoralens. One enduring question has been the following. What signals the synthesis of melanin or the reduction in psoriatic lesions in patients treated with psoralen plus UVA? A first step toward answering this question may have been provided by our present and previous work (Sastry & Hearst, 1991a,b). The inhibition of transcription initiation and elongation by cross-links may signal transcription-coupled repair systems (Friedberg, 1996; Sancar, 1996). Transcription-coupled repair may trigger the cascade of events in the clinical effects of psoralens. Previous workers showed that psoralen photoaddition inhibited *E. coli* RNAP initiation (Gnaizdowski et al., 1988, and references therein), but neither were the psoralens site-specific nor were the inhibitory steps identified.

ACKNOWLEDGMENT

Our special thanks are for Dr. Sean Cahill of the Spectroscopy Facility at the Rockefeller University for help with circular dichroism. We are grateful to Dr. John Helmann for his comments on an earlier version of this paper, to the two anonymous reviewers for helping us improve the presentation of the paper, and to Prof. Joshua Lederberg for his interest in the project.

REFERENCES

Alter, H. J., Creagan, R. P., Morel, P. A., Wiesehahn, G. P., Dorman, B. P., Corash, L., Smith, G. C., Popper, H., & Eichberg, J. W. (1988) *Lancet 2*, 1446−1450.

Basu, S., & Maitra, U. (1986) *J. Mol. Biol. 190*, 425−437.

Borukhov, S., Sagitov, V., Josaitis, C. A., Gourse, R. L., & Goldfarb, A. (1992) *J. Biol. Chem. 268*, 23477−23482.

Buc, H., & McClure, W. R. (1985) *Biochemistry 24*, 2712−2723.

Butzow, J. J., Oehrl, L. L., & Eichhorn, G. L. (1991) *Biochemistry 30*, 6454−6464.

Cantor, C. R., & Schimmel, P. (1980) *Biophysical chemistry. The behavior of biological macromolecules. Part III*, pp 855−863, W. H. Freeman, San Francisco.

Chamberlin, M. J., & Ryan, T. (1982) *Enzymes 15*, 87−108.

Chapman, K. A., & Burgess, R. R. (1987) *Nucleic Acids Res. 15*, 5413−5432.

Chapman, K. A., Gunderson, S. I., Anello, M., Wells, R. D., & Burgess, R. R. (1988) *Nucleic Acids Res. 16*, 4511−4524.

Cimino, G. D., Gamper, H., Isaacs, S. T., & Hearst, J. E. (1985) *Annu. Rev. Biochem. 54*, 1151−1193.

Cowing, D. W., Mecsas, J., Record, M. T., & Gross, C. A. (1989) *J. Mol. Biol. 210*, 521−530.

deHaseth, P. L., & Helmann, J. D. (1995) *Mol. Microbiol. 16*, 817−824.

Diaz, G. A., Raskin, C. A., & McAllister, W. T. (1993) *J. Mol. Biol. 229*, 805−811.

Diaz, G. A., Rong, M., McAllister, W. T., & Durbin, R. (1996) *Biochemistry 35*, 10837−10843.

Dunn, J. J., & Studier, F. W. (1982) *J. Mol. Biol. 166*, 477−535; *J. Mol. Biol.* (1984) *175*, 111−112 (erratum).

Friedberg, E. C. (1996) *Annu. Rev. Biochem. 65*, 15−42.

Gamper, H., Piette, J., & Hearst, J. E. (1984) *Photochem. Photobiol. 40*, 29 −34.

Gnaizdowski, M., Czyz, M., Wilmanska, D., Studzian, K., Frasunek, M., Plucienniczak, A., & Szmigiero, L. (1988) *Biochim. Biophys. Acta 950*, 346−353.

Grodberg, J., & Dunn, J. J. (1988) *J. Bacteriol. 170*, 1245−1253.

Gross, L., Chen, W. J., & McAllister, W. T. (1992) *J. Mol. Biol. 228*, 488−505.

Gunderson, S. I., Chapman, K. A., & Burgess, R. R. (1987) *Biochemistry 26*, 1539−1546.

Ikeda, R. A., Lin, A. C., & Clarke, J. (1992a) *J. Biol. Chem. 267*, 2640−2649.

Ikeda, R. A., Warshanna, G. S., & Chang, L. (1992b) *Biochemistry 31*, 9073−9080.

Ikeda, R. A., Chang, L. L., & Warshmanna, G. S. (1993) *Biochemistry 32*, 9115−9124.

Ivanov, V. I., Minchenkova, L. E., Schyolkina, A. K., & Poletayev, A. I. (1973) *Biopolymers 12*, 89−110.

Jia, Y., Kumar, A., & Patel, S. (1996) *J. Biol. Chem. 271*, 30451−30458.

Johnson, B. B., Dahl, K. S., Tinoco, I., Jr., Ivanov, V. I., & Zhurkin, V. B. (1981) *Biochemistry 20*, 73−78.

Jorgensen, E. D., Durbin, R. K., Risman, S. S., & McAllister, W. T. (1991) *J. Biol. Chem. 266*, 645−651.

Joyce, C. M., & Steitz, T. A. (1994) *Annu. Rev. Biochem. 63*, 777−822.

Joyce, C. M., & Steitz, T. A. (1995) *J. Bacteriol. 177*, 6321−6329.

Juang, Y.-L., & Helmann, J. D. (1995) *Biochemistry 34*, 8465−8473.

Kao, J. P.-Y. (1984) Ph.D. Thesis, University of California, Berkeley, CA.

Kornberg, A., & Baker, T. (1992) *DNA replication*, p 189, W. H. Freeman & Co., New York.

Kovacic, R. T. (1987) *J. Biol. Chem. 262*, 13654−13661.

Krummel, B., & Chamberlin, M. J. (1989) *Biochemistry 28*, 7829−7842.

Lin, L., Wiesehahn, G. P., Morel, P. A., & Corash, L. (1989) *Blood 74*, 517−525.

Lin, L., Londe, H., Hanson, C. V., Wisehahn, I. S., Cimino, G., & Corash, L. (1993) *Blood 82*, 292−297.

Ling, M. L., Risman, S. S., Klemant, J. F., McGraw, N., & McAllister, W. T. (1989) *Nucleic Acids Res. 17*, 1605−1681.

Maniatis, T., Fritsch, E. F., & Sambrook, J. (1982) *Molecular cloning: A laboratory manual*, pp 122, 148, Cold Spring Harbor Laboratory Press, Plainview, NY.

Martin, C. T., Muller, D. K., & Coleman, J. E. (1988) *Biochemistry 27*, 3966−3974.

Maslak, M., & Martin, C. (1993) *Biochemistry 32*, 4281−4285.

Maslak, M., & Martin, C. T. (1994) *Biochemistry 33*, 6918−6924.

Maslak, M., Jaworski, M. D., & Martin, C. (1993) *Biochemistry 32*, 4270−4274.

McAllister, W. T. (1993) *Cell. Mol. Biol. 39*, 385−391.

McAllister, W. T., & Carter, A. D. (1980) *Nucleic Acids Res. 8*, 4821−4837.

McClure, W. R. (1985) *Annu. Rev. Biochem. 54*, 171−204.

Mecsas, J., Cowing, D. W., & Gross, C. A. (1991) *J. Mol. Biol. 220*, 585−597.
Muller, D. K., Martin, C. T., & Coleman, J. E. (1988) *Biochemistry 27*, 5763−5771.
Muller, D. K., Martin, C. T., & Coleman, J. E. (1989) *Biochemistry 28*, 3306−3313.
Nelson, J. W., & Tinoco, I. J. (1984) *Biopolymers 23*, 213−233.
Osterman, H. L., & Coleman, J. E. (1981) *Biochemistry 20*, 4884−4892.
Pathak, M. A., & Fitzpatrick, T. B. (1992) *J. Photochem. Photobiol., B 14.*, 3−22.
Pavco, P., & Steege, D. A. (1991) *Nucleic Acids Res. 19*, 4639−4646.
Raskin, C. A., Diaz, G. A., Joho, K. E., & McAllister, W. T. (1992) *J. Mol. Biol. 228*, 506−515.
Rastinejad, F., & Lu, P. (1993) *J. Mol. Biol. 232*, 105−122.
Reardon, J. T., Speilmann, P., Huang, J. C., Sastry, S. S., Sancar, A., & Hearst, J. E. (1991) *Nucleic Acids Res. 19*, 4623−4629.
Reardon, J. T., Thompson, L. H., & Sancar, A. (1993) *Cold Spring Harbor Symp. Quant. Biol. 58*, 605−617.
Reisbig, R. R., Woody, A. Y., & Woody, R. W. (1979) *J. Biol. Chem. 254*, 11208−11217.
Roe, J. H., Burgess, R. R., & Record, M. T., Jr. (1985) *J. Mol. Biol. 184*, 441−453.
Saenger, W. (1984) *Principles of nucleic acids*, pp 385−431, Springer-Verlag, Berlin.
Sage, E., Drbetsky, E. A., & Moustacchi, E. (1993) *EMBO J. 12*, 397−402.
Sancar, A. (1995) *J. Biol. Chem. 270*, 15915−15918.
Sastry, S. S. (1996) *Biochemistry 35*,,13519−13530.
Sastry, S. S., & Hearst, J. E. (1991a) *J. Mol. Biol. 221*, 1091−1110.
Sastry, S. S., & Hearst, J. E. (1991b) *J. Mol. Biol. 221*, 1111−1125.
Sastry, S. S., & Ross, B. M. (1996) *Biochemistry 35*, 15715−15725.
Sastry, S. S., Spielmann, H. P., Dwyer, T. J., Wemmer, D. E., & Hearst, J. E. (1992) *J. Photochem. Photobiol., B 14*, 65−79.
Sastry, S. S., Spielmann, H. P., & Hearst, J. E. (1993a) *Adv. Enzymol. 66*, 85−148.
Sastry, S. S., Spielmann, H. P., Hoang, Q. S., Phillips, A. M., Sancar, A., & Hearst, J. E. (1993b) *Biochemistry 32*, 5526−5538.
Scaria, P., Will, S., Levenson, C., & Shafer, R. H. (1995) *J. Biol. Chem. 270*, 7295−7303.
Schick, C., & Martin, C. T. (1995) *Biochemistry 34*, 666−672.
Shi, Y.-B., Gamper, H., & Hearst, J. E. (1988) *J. Biol. Chem. 263*, 527−534.
Shimer, G. H., Jr., Woody, A.-Y., & Woody, R. W. (1988) *Biochim. Biophys. Acta 950*, 354−365.
Sousa, R., Patra, D., & Lafer, E. M. (1992) *J. Mol. Biol. 224*, 319−334.
Sousa, R., Chung, Y. J., Rose, J. P., & Wang, B.-C. (1993) *Nature (Lond). 364*, 593−599.
Spassky, A., Kirkegaard, K., & Buc, H. (1985) *Biochemistry 24*, 2723−2731.
Spielmann, H. P., Sastry, S. S., & Hearst, J. E. (1992) *Proc. Natl. Acad. Sci. U.S.A. 89*, 4514−4518.
Spielmann, H. P., Dwyer, T. J., Hearst, J. E., & Wemmer, D. E. (1995a) *Biochemistry 34*, 12937−12953.
Spielmann, H. P., Dwyer, T. J., Sastry, S. S., Hearst, J. E., & Wemmer, D. E. (1995b) *Proc. Natl. Acad. Sci. U.S.A. 92*, 2345−2349.
Stahl, S. J., & Chamberlin, M. J. (1978) *J. Biol. Chem. 253*, 4951−4959.
Suh, W.-C., Ross, W., & Record, M. T., Jr., (1992a) *Science 259*, 358−361.
Suh, W.-C., Leirmo, S., & Record, M. T., Jr. (1992b) *Biochemistry 31*, 7815−7825.
Tygarajan, K., Monfoerte, J., & Hearst, J. E. (1991) *Biochemistry 30*, 10920−10924.
Ujvari, A., & Martin, C. T. (1996) *Biochemistry 35*, 14574−14582.
Usattyi, A. F., & Shlayakhatenko, L. S. (1973) *Biopolymers 12*, 45−51.
Ussery, D. W., Hoepfner, R., & Sinden, R. R. (1992) *Methods Enzymol. 212*, 242−334.
Zawadzki, V., & Gross, H. J. (1991) *Nucleic Acids Res. 19*, 1948.

BI961793Y